Review on "Evaluation of Turbulent Flux Parameterizations over a Continental Glacier on the Tibetan Plateau"

This study presents the first comprehensive evaluation of turbulent flux parameterization schemes over a continental glacier on the Tibetan Plateau (TP), based on continuous eddy covariance (EC) observations collected at the Dunde Glacier from May to October 2023. The authors assess five representative turbulent flux schemes (C_{kat}, C_{log}, C_{Rib1}, C_{Rib2}, and C_{M-O}), analyze their performance across multiple temporal scales, and further evaluate their influence on glacier energy and mass balance simulations.

The topic is timely and significant, as turbulent fluxes are among the least constrained components of the surface energy balance on the TP, and direct EC observations over continental glaciers remain extremely rare. The manuscript is well structured, the data quality is high, and the results are clearly presented. The conclusions are supported by the analysis, and the discussion offers useful implications for improving glacier energy-balance modeling.

Overall, the paper provides valuable new insights into turbulent exchange processes over continental glaciers and represents a substantial contribution to TP glacier research. I recommend mayor revisions before publication.

Answer: We sincerely thank the Editor and the Reviewers for providing us with the opportunity to revise our manuscript. We are also grateful to the Reviewers for their constructive and valuable comments, which have greatly helped us improve the quality of the manuscript. All comments have been carefully addressed in the revised version. A point-by-point response to the comments from the Reviewer (highlighted in blue) is attached to this submission, along with the corresponding revisions in the manuscript (marked in brown). We believe that these revisions and clarifications have significantly improved the manuscript and made it suitable for publication.

Specific Comments

Abstract

1. Merely stating correlations is insufficient; are such correlations applicable across all glaciated regions? It is recommended that the authors explain with reference to the unique characteristics of the study area.

Answer: We agree with this important suggestion. In the revised manuscript, we have explicitly linked the observed turbulent flux characteristics to the specific environmental conditions of continental glaciers in the northeastern Tibetan Plateau, particularly in Section 4.1 (Results) and Section 5.1 (Discussion).

Specifically, we clarify that the Dunde Glacier is characterized by:

1. Low air temperature and low humidity conditions

2. A high-elevation observation site

3. A broad but generally low aerodynamic roughness length distribution

These features fundamentally distinguish it from maritime and sub-continental glacier environments. We have therefore emphasized in the Abstract that the findings are primarily representative of mid-latitude continental glacier environments on the Tibetan Plateau, rather than universally applicable to all glaciated regions.

The revised text is provided below:

L15: “Here, we present the first comprehensive analysis of turbulent flux characteristics and a systematic evaluation of turbulent flux methods for a continental glacier on the TP, using eddy covariance observations from the Dunde Glacier (May–October, 2023).”

L37: “These findings advance our knowledge of turbulent fluxes for continental glaciers on the TP and provide important guidance for the improvement of glacier models.”

L390: “Prevailing wind directions were westerly and northwesterly (Fig. 2m and o), highlighting the dominant influence of the mid-latitude westerlies on regional meteorological conditions.”

2. The abstract lacks a statement regarding the limitations of the study.

Answer: We appreciate this valuable suggestion. In the revised manuscript, we have explicitly acknowledged the main methodological and physical limitations of this study.

First, regarding turbulent flux calculation, we retain the 30 min averaging interval in this study in accordance with standard eddy-covariance processing protocols. However, we now explicitly acknowledge this choice as a methodological limitation. While 30 min averaging is widely adopted, it may smooth short-lived intermittent turbulence events over glacier surfaces. Future work will therefore explore shorter averaging intervals to better resolve intermittent turbulence and to assess its impact on turbulent flux estimates.

Second, we also clarify limitations related to the interpretation of turbulent flux behavior under extreme humid heatwave conditions. As discussed in the revised manuscript (Section 5.3), such events may cause continental glaciers to exhibit turbulent flux characteristics resembling those of maritime glaciers, including reduced LE magnitudes, occasional reversals in LE direction, and pronounced enhancement of H. However, this interpretation is likely influenced by the physical constraint that surface temperature (Ts) cannot exceed 0 °C. Under humid heatwave conditions, air temperature continues to rise while Ts is capped at the melting point, increasing the surface temperature deficit and enhancing H. Because the humidity gradient is closely coupled to the temperature gradient, LE may also undergo anomalous changes.

We now explicitly state that these mechanisms require further observational and modeling investigation. Additional multi-season and high-temporal-resolution measurements will be necessary to fully resolve turbulent processes under extreme meteorological conditions.

The revised text is provided below:

L727: “Under ongoing global warming, the climate system is recording notable warming and moistening trends on the TP (Wang et al., 2010). This means that the TP will likely experience an increased frequency and intensity of humid heatwave events

(Zhang et al., 2025). Such conditions will cause continental glaciers, such as the Dunde Glacier, to increasingly exhibit turbulent flux characteristics that resemble those of maritime glaciers, including reduced LE magnitudes and even reversals in LE direction, as well as a pronounced enhancement of H. This phenomenon warrants further investigation and is likely related to the constraint that T_s cannot exceed 0 °C. Under humid heatwave conditions, T_a continues to rise while T_s is capped, leading to an increased surface temperature deficit and consequently a substantial enhancement of H. Meanwhile, because the humidity gradient is closely coupled to the temperature gradient, LE may also undergo anomalous changes. Consequently, continued warming may drive future transitions in glacier types."

3. Why was the Dunde Glacier selected? In other words, what is the significance or importance of this glacier within the study region?

Answer: We have clarified this point in both the Introduction and Section 2.1.

The Dunde Glacier was selected because:

1. It is a typical mid-latitude continental glacier in the northeastern TP.

2. It is strongly influenced by the westerlies and characterized by cold and relatively dry conditions.

3. Continental glaciers are among the most widely distributed glacier types on the TP but remain severely under-observed in terms of turbulent flux measurements.

4. The glacier has established AWS and EC infrastructure, allowing sustained micrometeorological measurements.

These aspects highlight its regional representativeness and scientific importance. The revised text is provided below:

L64: "However, to date, there have been no reported observations of turbulent fluxes over continental glaciers on the TP characterized by low temperatures and precipitation, one of the most widely distributed glacier types on the TP. This data gap has resulted in an inadequate understanding of the relative contributions of individual energy balance components to the overall surface energy budget of TP glaciers, which,

in turn, is crucial for understanding the weather patterns controlling glacier variations across the TP."

1 Introduction

1. Although it already mentions "the first comprehensive analysis for a continental glacier," it is suggested to emphasize the differences and scientific significance of this study compared with existing research on maritime and sub-continental glaciers, preferably in the last one or two sentences.

Answer: We clearly state that parameterizations validated for maritime glaciers cannot be directly transferred to continental glaciers without observation-based evaluation. This reinforces the novelty of providing the first systematic EC-based evaluation for a continental glacier on the TP. The revised text is provided below:

L64: "However, to date, there have been no reported observations of turbulent fluxes over continental glaciers on the TP characterized by low temperatures and precipitation, one of the most widely distributed glacier types on the TP. This data gap has resulted in an inadequate understanding of the relative contributions of individual energy balance components to the overall surface energy budget of TP glaciers, which, in turn, is crucial for understanding the weather patterns controlling glacier variations across the TP."

2. It is recommended to slightly shorten the review of previous studies (lines 64–91) and instead expand the final paragraph to highlight the study's specific aims and hypotheses, ensuring a smooth logical transition into Section 2.

Answer: We streamlined the literature review (Lines 64–91 in the previous version) by removing redundant descriptions of previous modeling studies. We expanded the final paragraph to clearly articulate the study aims: "Here we provide the first systematic analysis of meteorological and glacier mass balance observations and direct

eddy-covariance-based turbulent flux measurements at the Dunde Glacier in the Qilian Mountains, the northeastern TP, to evaluate the applicability of multiple widely used turbulent flux methods over continental glaciers on the TP. We systematically analyze observed and modeled turbulent fluxes across multiple temporal scales, including daily mean, daily, and notably under extreme weather conditions, to test the performance of the turbulent flux models. Finally, we assess the influence of the various turbulent flux parameterizations on the simulated glacier mass balance by implementing the parameterizations in the energy and mass balance model. The findings allow us to improve the accuracy of glacier surface energy and mass balance modeling and to advance our understanding of ablation processes on continental glaciers on the TP."

The revised text is provided below:

L70: "Owing to the scarcity of observational data, numerical modeling is the primary method by which glacier turbulent fluxes have been estimated on the TP (Yang et al., 2011; Mölg et al., 2012; Zhu et al., 2018). Current turbulent flux modeling approaches predominantly rely on Monin–Obukhov similarity theory (MOST) (Monin and Obukhov, 1954), which has been widely applied for parameterizing near-surface turbulent fluxes. However, its performance over glaciers remains uncertain, particularly under strongly stable stratification and katabatic flow conditions, where the fundamental assumption of vertically constant turbulent fluxes is frequently violated (Grisogono et al., 2007). In addition to sophisticated turbulent flux models that strictly implement MOST (Yang et al., 2002; Hock and Holmgren, 2005), various simplified turbulent flux parameterizations have been developed to derive LE and H. To improve computational efficiency, Oerlemans (2000) applied a highly simplified bulk formulation to estimate near-surface turbulent fluxes, assuming logarithmic vertical profiles of wind speed, temperature, and humidity to be valid under prevailing stable conditions, without explicitly accounting for stability-dependent flux modifications. Essery and Etchevers (2004) and Suter et al. (2004) implemented stability correction functions based on the bulk Richardson number (Rib) to modify turbulent flux estimates within bulk aerodynamic methods. Oerlemans and Grisogono (2002) developed a turbulent flux model adapted to local glacier climatic conditions, which considers the

influence of glacier wind on turbulent fluxes. As a result, turbulent flux estimates for the same glacier can differ substantially depending on the choice of turbulent flux parameterization (Radić et al., 2017). Previous studies on the Zhadang Glacier clearly demonstrate this model-dependent variability, showing that the estimated multi-year mean turbulent heat fluxes for both winter and summer differ substantially when different modeling approaches are applied. Zhang et al. (2016) employed a highly simplified Monin–Obukhov–based bulk approach with constant exchange coefficients driven by near-surface wind speed and derived multi-year mean turbulent heat fluxes of 13.4 W m^{-2} in winter and 5.7 W m^{-2} in summer for the period 2011–2014. In contrast, Huintjes et al. (2015) adopted a bulk method in which atmospheric stability is represented by the bulk Richardson number, yielding multi-year mean turbulent heat fluxes of 8.0 W m^{-2} in winter and −28 W m^{-2} in summer during 2001–2011. Such differences may partly arise from variations in the study periods; However, a more important factor is the limited availability of observational data for calibrating turbulent flux parameterizations, as well as differences among the turbulent flux models themselves. Consequently, evaluations of the accuracy of different turbulent flux parameterizations over the TP remain limited, are largely confined to short time scales, and are constrained by the scarcity of EC observations. Moreover, comprehensive assessments of turbulent-flux schemes specifically for continental glaciers are still lacking. Guo et al. (2011) evaluated three turbulent flux parameterizations for the Parlung No.4 Glacier (maritime glacier) and found that the scheme proposed by Yang et al. (2002) produced lower errors in turbulent flux estimates during both individual melt phases and the entire ablation season. Compared with the other two schemes evaluated (Andreas, 1987; Smeets and van den Broeke, 2008), the mean absolute deviation (MAD) was reduced by approximately 12–29%. Liu et al. (2024) employed eddy-covariance measurements to validate a one-camera time-lapse structure-from-motion (O-T-SfM) photogrammetry approach for monitoring snow sublimation on the August-one ice cap. The results indicate that, under snow-free conditions, glacier surface sublimation rates estimated using the O-T-SfM method were in good agreement with EC measurements. Both methods successfully captured daily snow sublimation

during the winter season. However, to date, no comprehensive analysis has been conducted specifically for continental glaciers. Previous assessments focusing on maritime glaciers on the TP cannot be directly applied to the widely distributed continental glaciers due to fundamental differences in glacier characteristics. Continental glaciers therefore require observation-based evidence that is more directly applicable to their climatic and surface conditions (Zhu et al., 2023)."

Minor language point:

1. change "the important reasons of such difference are…" to "the main reason for such differences is…".

Answer: We thank the reviewer for this helpful correction. We have revised the language to improve clarity and grammatical accuracy. The modified sentence (L95) now reads:

"However, a more important factor is the limited availability of observational data for calibrating turbulent flux parameterizations, as well as differences among the turbulent flux models themselves."

This revision improves precision and readability.

2. Minor grammatical and stylistic edits are needed (e.g., "Here we provide the first systematically analyze…" → "Here we provide the first systematic analysis…").

Answer: We revised the phrasing to "systematic analysis" as suggested to improve clarity and stylistic consistency. The revised sentence **(L116)** now reads: "Here we provide the first systematic analysis of meteorological and glacier mass balance observations and direct eddy-covariance-based turbulent flux measurements at the Dunde Glacier…"

2 Study Area and Data

1. Figure 1 is informative, but panel (b) should include a scale bar, north arrows, which would help readers better understand the actual size and spatial extent of the Dunde Glacier.

Answer: We have revised Figure 1(b) to include both a scale bar and north arrow to improve spatial interpretability of the Dunde Glacier topography and station locations.

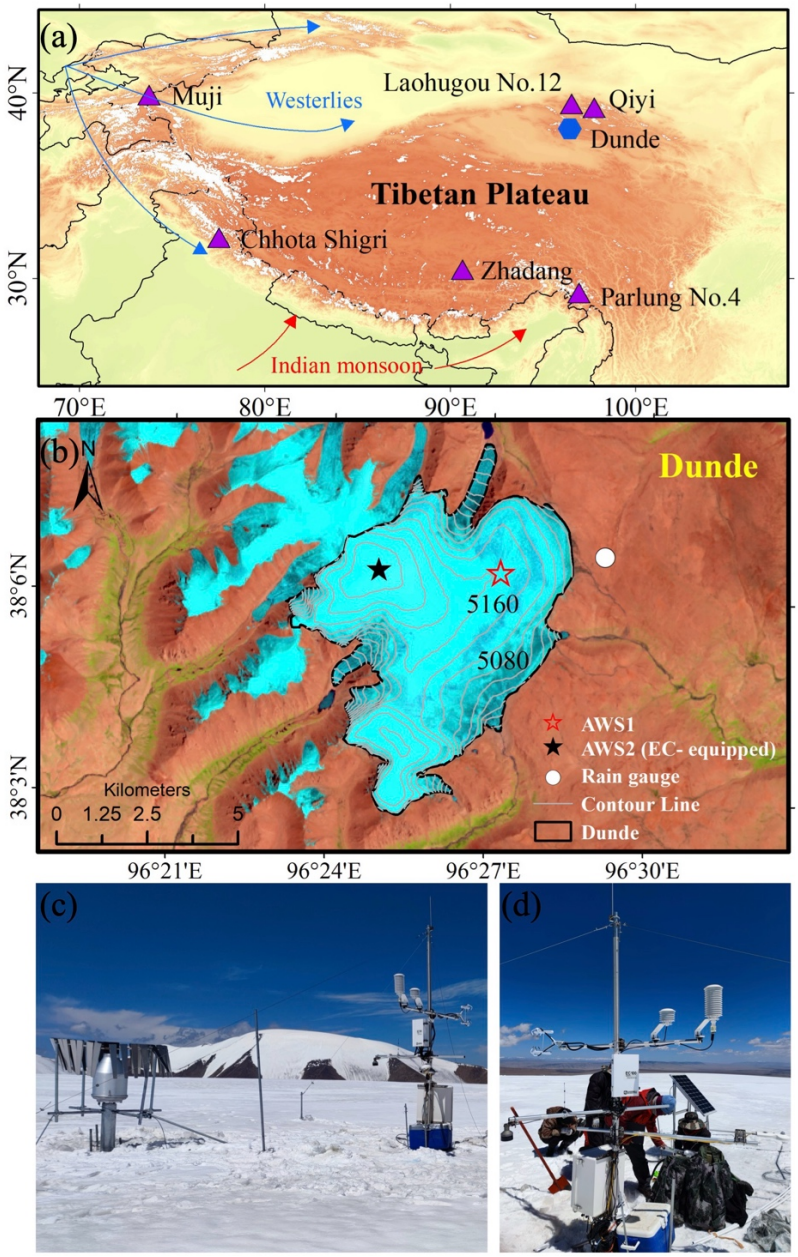

2. The authors might briefly explain why the Dunde Glacier was selected—for example, its representativeness of mid-latitude continental glacier conditions, the logistical advantages for EC deployment, and its climatic relevance to the Qilian Mountains.

Answer: We thank the reviewer for this suggestion. In the revised manuscript, we have provided a more comprehensive description of the Dunde Glacier in the Study Area and Data section. Specifically, we now detail:

1. Its geographical location in the northeastern Tibetan Plateau and its representativeness of mid-latitude continental glacier conditions;

2. Its climatic characteristics, including low temperature, relatively low precipitation, and strong influence of the westerlies;

3. Its documented glacier mass balance and long-term change characteristics;

4. Its hydrological significance for downstream rivers in the Qilian Mountains region.

In addition, we provide a detailed description of the observational infrastructure installed on the glacier, including: The eddy covariance (EC) system; Multiple automatic weather stations (AWS); Precipitation gauges; The measured meteorological and turbulence variables and their installation heights and locations.

These additions clarify both the scientific representativeness and the observational suitability of the Dunde Glacier for this study.

The revised text is provided below:

L128: "2.1. Measurement site

The Dunde Glacier is located in the western part of the Qilian Mountains, on the Northeastern TP. It is a typical continental glacier, with an elevation ranging from 4400 to 5500 m (Guo et al., 2015). The ice cap covers an area of approximately 60 km², with an average annual elevation change rate of -0.501 ± 0.08 m yr^{-1} (Hugonnet et al., 2021). The region experiences pronounced annual and daily temperature variations, with a mean annual temperature of approximately −5 °C and annual precipitation ranging from 300 to 400 mm. Meltwater from the glacier primarily feeds into the Tataleng and

Haerteng rivers, which provide an important water source to their respective drainage basins. The observation site was situated on the surface of the Dunde Glacier (38°06′23″ N, 96°24′54″ E) at an elevation of 5,317 m a.s.l., as shown in Fig. 1, and served as the primary observation site for this study."

L147: "2.2. Meteorological data

Meteorological variables, including air temperature, air pressure, relative humidity, wind speed and direction, incoming and outgoing shortwave radiation, incoming and outgoing longwave radiation, and glacier surface height, were primarily measured at the study site using a Campbell-ClimaVUE50 automatic weather station (AWS1) located at 5317 m a.s.l. To ensure temporal continuity, occasional data gaps in these variables were filled using linear interpolation based on observations from a nearby auxiliary station (AWS2). The glacier surface temperature used in this study was derived from the observed outgoing longwave radiation, assuming a constant surface emissivity of 0.98. Details of the sensors used to measure each variable are provided in Table 1."

L167: Table 1: Characteristics of the sensors installed in the eddy covariance system to measure turbulent fluxes and meteorological variables in this study.

Variable	Symbol (unit)	Sensor	Accuracy	Range	Height
Air temperature	T_a (°C)	Vaisala HMP155A	20 to 60 °C: ± (0.055 + 0.0057×T_a) °C −80 to 20 °C: ± (0.226 − 0.0028×T_a) °C	−80 to 60 °C	2.17 m
Relative humidity	RH (%)	Vaisala HMP155A	± 2%	0%–100%	2.17 m
Wind speed	u (m s^{-1})	LICOR LI-7500DS	± 1.5%	0–100 m s^{-1}	2.05 m
Wind direction	WD (°)	LICOR LI-7500DS	± 2º	360 º	2.05 m
Air pressure	P (Pa)	Vaisala PTB210	± 0.5 hPa	50–1100 hPa	2.05 m
Incoming and outgoing longwave radiation	LWI, LWO (W m^{-2})	Campbell CNR4	± 1%	−250 to 250 W m^{-2}	1.60 m

Incoming and outgoing shortwave radiation	SWI, SWO (W m^{-2})	Campbell CNR4	± 1%	0–2000 W m^{-2}	1.60 m
Turbulent wind components	u′, v′, w′ (m s^{-1})	3-D sonic anemometer (Campbell IRGASON / CSAT3)	±1 mm s^{-1} (u′, v′) ±0.5 mm s^{-1} (w′)	0–65 m s^{-1}	2.05 m
Precipitation	(mm)	Geonor T-200B	± 0.1% Full Scale	0–600 mm	1.70 m

L170: "2.3. Eddy-Covariance systems

Turbulent fluxes were measured with a CSAT3 three-dimensional sonic anemometer (Campbell IRGASON) and subsequently processed using the eddy covariance (EC) method during the period from 14 May to 12 October 2023; this is a widely adopted technique in micrometeorological research that enables real-time, accurate, and continuous monitoring of atmospheric turbulence. All turbulence raw data were collected at 10 Hz, including the three components of wind velocity, virtual temperature, and water vapor concentration."

3. Please amend the elevation "5317 m" to the standard format "5,317 m".

Answer: We thank the reviewer for pointing out this formatting issue. We have corrected "5317 m" to "5,317 m" in accordance with journal formatting conventions. In addition, we carefully reviewed the entire manuscript and ensured that all elevation values and numerical expressions are now consistently formatted throughout the text. The revised text is provided below:

L134: "The observation site was situated on the surface of the Dunde Glacier (38°06′23″ N, 96°24′54″ E) at an elevation of 5,317 m a.s.l., as shown in Fig. 1, and served as the primary observation site for this study."

L148: "Meteorological variables, including air temperature, air pressure, relative humidity, wind speed and direction, incoming and outgoing shortwave radiation, incoming and outgoing longwave radiation, and glacier surface height, were primarily measured at the study site using a Campbell-ClimaVUE50 automatic weather station (AWS1) located at 5,317 m a.s.l."

3 Methods

1. Section 3 is comprehensive but quite dense due to numerous equations. It is strongly suggested to include a summary table comparing the five schemes (C_{kat}, C_{log}, C_{Rib1}, C_{Rib2}, $C_{M–O}$) in terms of (a) stability correction, (b) iterative requirement, and (c) computational complexity. This would greatly enhance clarity and help readers grasp their physical and numerical distinctions.

Answer: We appreciate the reviewer's suggestion. In the revised manuscript, we have carefully restructured and clarified the Methods section to improve logical transparency and readability.

Specifically, we now present a clearer logical workflow beginning with the Clog method as the baseline bulk formulation. From this starting point, the subsequent methods (CRib1, CRib2, CM–O, and Ckat) are introduced in a progressive manner, explicitly clarifying the differences among the schemes in their treatment of atmospheric stability corrections.

To further support reproducibility, we provide a comprehensive parameter table summarizing all physical constants, empirical coefficients, and model-specific parameters used in the study.

Through these revisions, the methodological structure has been streamlined, the logical progression among bulk schemes has been made more explicit, and the reproducibility of the modeling framework has been strengthened.

The revised text **(L239)** is provided below:

"**3.2 Bulk methods**

Variations in the performance of different turbulent flux parameterizations primarily arise from their respective approaches to computing turbulent exchange coefficients and applying atmospheric stability corrections. These methodological differences directly affect method accuracy under varying temperature gradients, humidity gradients, and wind speed conditions, leading to discrepancies in the simulated LE and H. In this study, we evaluate two categories of bulk aerodynamic

methods for calculating turbulent fluxes over glacier surfaces. The first category comprises methods in which the bulk exchange coefficient (C) is formulated as a function of surface roughness lengths and atmospheric stability. The second category includes bulk methods that explicitly incorporate a simplified katabatic (glacier wind) parameterization.

Within this framework, we analyze five bulk methods that are commonly applied to glacier surfaces. These include: (i) a simplified bulk formulation without explicit stability corrections (C_{log}); (ii) and (iii) bulk methods that account for atmospheric stability through the bulk Richardson number (C_{Rib1} and C_{Rib2}); (iv) a method based on the full Monin–Obukhov similarity theory, employing universal stability functions with iterative closure (C_{M-O}); and (v) a bulk method derived from a simplified katabatic flow model that explicitly considers glacier wind effects (C_{kat}). The detailed formulations of methods (i) through (v) are described in the following subsections.

Model performance is evaluated by comparing 30-min turbulent fluxes (H and LE) simulated by each method with eddy covariance (EC) measurements, using standard statistical metrics including the root mean square error (RMSE), mean bias error (MBE), and mean absolute deviation (MAD). For consistency between modeled and observed fluxes, turbulent fluxes are defined as positive when directed from the atmosphere toward the glacier surface, and negative in the opposite direction. The naming of the turbulent flux methods follows the convention of Radić et al. (2017).

3.2.1. C_{kat} method

The C_{kat} method explicitly considers katabatic flows, introducing the katabatic bulk exchange coefficient (C_{kat}) to partially overcome the limitations of MOST during strong katabatic wind conditions (Oerlemans and Grisogono, 2002). This approach emphasizes intensified katabatic turbulence during nocturnal cooling or cold-air intrusions, enhancing turbulent exchange (Horst and Doran, 1988). However, the C_{kat} method lacks explicit stability corrections and dynamic roughness length adjustment, leading to a slow response under rapidly changing surface conditions (Denby, 2000).

Hence, its application is more suited to small and medium-sized glaciers rather than large-scale domains. LE and H are expressed as:

$$LE = \frac{0.622}{P}\rho L_{s/f}\mathrm{C_{kat}}(e_a - e_s), \quad (7)$$

$$H = \rho \mathrm{C_P C_{kat}}(T_a - T_s), \quad (8)$$

where, ρ and C_P are the density (kg·m^{-3}) and heat capacity of air, respectively; P is atmospheric pressure (Pa), $L_{s/f}$ is the latent heat of sublimation/fusion, selected based on surface temperature; e_a and $\mathrm{e_s}$ are the atmospheric vapor pressure and saturated vapor pressure at the glacier surface (Pa), respectively; T_a and T_s denote the air temperature and glacier surface temperature, respectively; and C_{kat} is the katabatic bulk exchange coefficient, calculated using the following equation:

$$\mathrm{C_{kat}} = -C_{tub}C_{tub_2}^2 C\left(\frac{g}{T_0 \gamma P_r}\right)^{1/2}, \quad (9)$$

Here, C_{tub} and C_{tub2} are dimensionless empirical constants used to optimize the parameterization of turbulent fluxes; C is replaced by the air–surface temperature difference ($\mathrm{T_a}$–$\mathrm{T_s}$); T_0= 273.15 K; γ is the potential temperature gradient, which is prescribed as a constant value of 0.005 K m^{-1} (Oerlemans and Grisogono, 2002); and P_r is the Prandtl number (~ 0.71).

3.2.2. $\mathrm{C_{log}}$ method

The $\mathrm{C_{log}}$ method represents a highly simplified derivative of MOST. This method employs a constant exchange coefficient (C_h) driven by near-surface wind speed and the difference in air temperature (or humidity) and surface temperature (or humidity), providing a simplified, computationally efficient structure suitable for large-scale climate models (Oerlemans, 2000). It does not dynamically adjust atmospheric stability, and instead retains only a linear relationship for surface fluxes. Being a wind-speed-driven scheme, it performs well under less stable stratification conditions. However, the method also exhibits certain limitations. Owing to the absence of atmospheric stability parameters in its structure, it cannot identify or respond to surface inversions forming at night or in the early morning. LE and H are expressed as:

$$LE = 0.622\rho L_{s/f} C_h u(e_a - e_s)/P, \quad (10)$$

$$H = \rho C_P C_h u(T_a - T_s), \quad (11)$$

where, u is wind speed (m·s^{-1}), and C_h is the turbulent exchange coefficient. Following (Oerlemans, 2000), turbulent fluxes are regulated through the exchange coefficient C_h. Here, C_h is treated as a calibration parameter and optimized by minimizing the mismatch between modeled and observed turbulent fluxes.

3.2.3. C_{Rib1} method

The C_{Rib1} method retains the C_{log} formulation for turbulent flux calculation but introduces the bulk Richardson number (Rib) to allow for flux reduction under stable stratification (Suter et al., 2004). The bulk Richardson number can be related to the stability functions for momentum (ϕ_m), heat (ϕ_h), and water vapour (ϕ_q) in the following way ((Oke, 1987); see Eq. 14). In this formulation, the composite function ($f_h(Ri_b)$) is constructed from the stability functions for momentum (ϕ_m), heat (ϕ_h), and water vapor (ϕ_q) (Dyer, 1974; Holtslag and Bruin, 1988).

$$LE = \rho L_{s/f} \kappa^2 z_u z_q \left(\frac{\Delta\bar{u}\Delta\bar{q}}{z^2}\right)(\phi_m\phi_h)^{-1}, \quad (12)$$

$$H = \rho C_P \kappa^2 z_u z_t \left(\frac{\Delta\bar{u}\Delta\bar{T}}{z^2}\right)(\phi_m\phi_q)^{-1}, \quad (13)$$

$$\begin{cases} (\phi_m\phi_{h,q})^{-1} = (1 - 5Ri_b)^2 & (Ri_b > 0) \\ (\phi_m\phi_{h,q})^{-1} = (1 - 16Ri_b)^{0.75} & (Ri_b \le 0) \end{cases}, \quad (14)$$

$$Ri_b = \frac{g\frac{\Delta\bar{T}}{\Delta Z}}{\bar{T}\left(\frac{\Delta\bar{u}}{\Delta Z}\right)^2}, \quad (15)$$

where, $\bar{u}$, $\bar{q}$, and $\bar{T}$ represent the mean wind speed, specific humidity, and air temperature, respectively; where $z_{u,t,q}$ are the log mean heights defined as:

$$z_{u,t,q} = \frac{z - z_{0u,t,q}}{ln\left(\frac{z}{z_{0u,t,q}}\right)}, \quad (16)$$

and $z_{0u,q,t}$ denotes the surface roughness lengths for momentum, humidity, and temperature.

3.2.4. C_{Rib2} method

Similar to C_{Rib1}, the C_{Rib2} method is a non-iterative method for calculating turbulent fluxes (Essery and Etchevers, 2004). It employs Ri_b and $f_h(Ri_b)$, thereby reducing computational complexity while preserving the physical consistency of MOST. Turbulent fluxes in the C_{Rib2} method are calculated as:

$$LE = \rho L_{s/f} C_H u[q_{sat}(T_s, P) - q], \tag{17}$$

$$H = \rho C_P C_H u[T_s - T_a], \tag{18}$$

where, $q_{sat}(T_s, P)$ denotes the saturation specific humidity at surface temperature T_s and pressure P, and C_H is a surface exchange coefficient. Following Essery and Etchevers (2004) and Louis (1979), the exchange coefficient for surface sensible and latent heat flux is calculated as $C_H = C_{Hn} f_h$, where

$$C_{Hn} = \kappa^2 \left[\ln\left(\frac{z}{z_{0m}}\right)\right]^{-2}, \tag{19}$$

is the neutral exchange coefficient for roughness length $z_{0\mathrm{m}}$ and

$$f_h = \begin{cases} (1 + 10Ri_b)^{-1} & Ri_b \geq 0 \\ 1 - 10Ri_b\left(1 + 10Ri_b C_{Hn}\sqrt{-Ri_b}/f_z\right)^{-1} & Ri_b < 0 \end{cases}, \tag{20}$$

with

$$f_z = \frac{1}{4}\left(\frac{z_{0m}}{z}\right)^{1/2}, \tag{21}$$

Although atmospheric stability is also characterized by Ri_b, the calculation approach in C_{Rib2} method differs from that in C_{Rib1} method as follows:

$$Ri_b = \frac{g z_1}{u^2}\left\{\frac{T_a - T_s}{T_a} + \frac{q - q_{sat}(T_s, P)}{q + \epsilon/(1-\epsilon)}\right\}, \tag{22}$$

where, ϵ is defined as the ratio of the molecular weights of water to dry air, with a value of 0.622.

3.2.5. C_{M-O} method

This method replaces the composite stability function $f_h(Ri_b)$ used in the C_{Rib} with the universal stability functions (ψ) to introduce stability corrections. It adopts a complete MOST framework and explicitly calculates the friction velocity (u^*), ψ, and L (Hock and Holmgren, 2005). Separate roughness lengths are applied for momentum

(z_{0m}), temperature (z_{0t}) and humidity (z_{0e}). Turbulent fluxes are obtained through an iterative solution procedure that ensures closure of the nonlinear stability equations.Under stable conditions, the nonlinear stability functions of Beljaars and Holtslag (1991) are used, whereas under unstable conditions, the Businger–Dyer relationships are applied (Beljaars and Holtslag, 1991; Paulson, 1970). The variables $u*$ and L solved iteratively to achieve convergence.

$$LE = L_{s/f}\frac{0.622\rho}{P_0}\frac{k^2}{\left[\ln\left(\frac{z}{z_{0m}}\right)-\psi_M\left(\frac{z}{L}\right)\right]\left[\ln\left(\frac{z}{z_{0e}}\right)-\psi_E\left(\frac{z}{L}\right)\right]}u(e_a - e_s), \quad (23)$$

$$H = \rho C_P\frac{k^2}{\left[\ln\left(\frac{z}{z_{0m}}\right)-\psi_M\left(\frac{z}{L}\right)\right]\left[\ln\left(\frac{z}{z_{0t}}\right)-\psi_H\left(\frac{z}{L}\right)\right]}u(T_a - T_s)\ , \quad (24)$$

For clarity and reproducibility, all model-specific parameters and physical constants used in this study are summarized in Table 2, together with their numerical values, units, and data sources where applicable."

Table 2: Summary of model-specific parameters and physical constants adopted in this study.

Parameter	Description	Value	Unit	Source
C_{turb}	dimensionless empirical constants	0.0001	–	this study
C_{turb2}	dimensionless empirical constants	0.007	–	this study
γ	potential temperature gradient	0.005	K m^{-1}	Oerlemans and Grisogono, 2002
P_r	Prandtl number	0.71	–	Standard value
$L_{s/f}$	latent heat of sublimation/evaporation	$L_f = 2.514\times10^6$ $L_s = 2.849\times10^6$	J kg^{-1}	Standard value
Cp	heat capacity of air	1005	J kg^{-1} K^{-1}	Standard constant
C_h	turbulent exchange coefficient (recalibrated in this study)	0.0005	–	this study
C_h	turbulent exchange coefficient (reference value)	0.00127	–	Oerlemans, 2000
κ	von Karman constant	0.4	–	Standard constant
P_0	mean atmospheric pressure at sea level	101325	Pa	Standard value
z_0	Aerodynamic roughness length (literature value)	0.003	m	Essery and Etchevers, 2004

z_{0m}	Aerodynamic roughness length (literature value)	0.01	m	Hock and Holmgren, 2005

2. Check the consistency of formula expressions — for example, ensure that the pressure variable symbols used in Equations (4), (11), and (16) and Table 2, as well as the air pressure notation in Section 4.1, remain consistent throughout the manuscript.

Answer: We carefully checked all formula expressions and ensured that pressure notation is consistent across Equations (4), (11), (16), Table 2, and Section 4.1.

4 Results

In Sections 4.3.1 and 4.3.2, add a brief summary sentence at the end of each paragraph to highlight which method performs best overall for each flux (LE and H), and indicate which scheme performs best in different seasons.

We thank the reviewer for this constructive suggestion. Following a revision of the data screening procedure, the observational dataset used for model evaluation became temporally discontinuous and was primarily concentrated during the ablation season. As a result, seasonal segmentation no longer provided statistically robust comparisons. Therefore, we removed the former Section 4.3.2 (seasonal comparison) and instead focused on two more reliable evaluation scales: the overall study period and diurnal variations.

In each relevant subsection, we now explicitly describe the relative performance of the different turbulent flux schemes. Furthermore, at the end of Section 4.3, we provide a comprehensive summary that clearly states:

- Which turbulent flux methods perform best over the entire study period;
- Which methods better reproduce diurnal variability;
- Which scalar roughness length parameterization (A87 or SvdB) demonstrates superior performance.

These revisions ensure that model performance is clearly synthesized while remaining consistent with the statistical robustness of the available observational data.

The revised text **(L546)** is provided below:

"In summary, among the five evaluated methods, both the C_{kat} and C_{log} schemes exhibited a tendency to underestimate the observed turbulent fluxes to some extent; however, the optimized parameters adopted in these schemes provide useful references for studies of continental glaciers. For the EC-based approaches derived from observations (i.e., the C_{Rib1}, C_{Rib2}, and C_{M-O} methods), the overall performance in simulating both LE and H was broadly comparable throughout the study period, with generally higher simulation accuracy for H than for LE. Nevertheless, differences among the schemes became more evident when examining the diurnal variations. In particular, the C_{Rib1} and C_{Rib2} methods showed closer agreement with observations in reproducing the diurnal evolution of LE, whereas the differences among schemes in simulating H were relatively small. In addition, considering both the overall period and the diurnal cycle, the SvdB scalar roughness length parameterization consistently outperformed the A87 scheme. Overall, although the differences among the five schemes were not substantial, the methods employing Richardson number-based stability corrections combined with the SvdB scalar roughness parameterization demonstrated comparatively balanced performance in simulating both LE and H, and were able to more accurately reproduce the diurnal evolution of turbulent fluxes. Therefore, among the five evaluated schemes, this class of approaches can be regarded as a relatively favorable option for simulating turbulent fluxes over the Dunde Glacier. More broadly, it may also be applicable to turbulent flux simulations over continental glaciers on the TP."

5 Discussion

1. In Section 5.2, the authors should clearly specify the data required and their sources for the energy balance–snow and firn model used in this study, and indicate whether

these details have been sufficiently provided in the Study Area and Data section. The model output variables should also be explicitly described.

Answer: We thank the reviewer for pointing out this ambiguity. The term "recalibrated parameters" indeed refers to parameters within the energy-balance and mass-balance framework (EBFM), and we agree that this needs to be clearly explained in the Methods.

In the revised manuscript, we have substantially expanded the description of the EBFM in Section 3.3, where all calibrated parameters and their roles in the surface energy balance are explicitly defined. In addition, Section 5.2 now clearly specifies the sources of all input variables used to drive the EBFM, including how surface temperature T_s is determined within the model framework.

These revisions are intended to ensure that the only varying component influencing the EBFM simulations in the sensitivity experiments is the choice of turbulent flux parameterization, while all other inputs and model parameters are treated consistently. This clarification resolves the ambiguity regarding the meaning of "recalibrated parameters" and provides a transparent basis for interpreting the modeled surface temperature and mass-balance responses.

The revised sentence **(L349 and L609)** now reads:

L349: "3.3 Energy Balance Model

The approximate SEB (in W m^{-2}) can be written as:

$$Q_m = S_{\text{in}} + S_{\text{out}} + L_{\text{in}} + L_{\text{out}} + H + LE + Q_{\text{rain}} + Q_{\text{sub}} \ , \quad (25)$$

where Q_m is the energy available for melt, S_{in} represents the incoming shortwave radiance, S_{out} is the reflected shortwave radiation, and L_{in} and L_{out} refer to the incoming and outgoing longwave radiation, respectively. Q_{rain} is the heat transfer due to rainfall, while Q_{sub} denotes the heat flux into the ice. In the model, the energy fluxes are expressed in a way that the surface temperature is the only unknown variable, which is determined by iteratively solving Eq. (25) with the left-hand-side set to zero. If the computed surface temperature exceeds the melting point, it is constrained to the melting point, and the energy fluxes are recalculated. In this scenario, the sum of fluxes becomes

positive, and melting will occur (EBFM; Van Pelt et al., 2012, 2019). The mass balance (MB, mm w.e.), is calculated as follows:

$$MB = \int \left(\frac{Q_m}{L_m} + P_{snow} + \frac{Q_L}{L_s}\right) dt\,, \quad (26)$$

P_{snow} is the snow accumulation, Q_L is the mass exchange due to sublimation. L_m is the latent heat of melting (~ 3.34×10^5 J kg^{-1}). Since this study is based on point data and does not involve spatial data, topographical parameters were not set in EBFM during the analysis."

L609: **"5.2 Performance improvement of the SEB model by optimizing turbulent flux methods**

To assess the importance of turbulent flux methods in simulating glacier mass balance, we included three representative turbulent flux methods (the C_{log}, C_{Rib2}, and C_{M-O} + SvdB methods) in a coupled energy balance–snow and firn model applied at the point scale. For each method, turbulent fluxes were computed using both the original parameter sets reported in the literature and the recalibrated parameters developed in this study, while all other model inputs, including incoming and outgoing longwave radiation, incoming and outgoing shortwave radiation, snow depth, surface albedo, and rainfall, were prescribed from in situ observations at AWS1 to ensure a controlled experimental setup."

2. In Section 5.3, Are the specific dates shown confirmed to represent extreme high temperature events? The authors should clearly describe the criteria used to identify extreme weather and climate events.

Answer: We thank the reviewer for this important comment. In the revised manuscript, we have clarified the criteria used to identify the humid heatwave event.

Specifically, the identification of extreme events was based on a comparison with climatological conditions during the same calendar period in different years. Rather than relying solely on air temperature and relative humidity, we calculated wet-bulb

temperature (Tw), which integrates both air temperature and humidity and is therefore more physically relevant for assessing glacier surface energy exchange under humid conditions.

An event was classified as extreme when the calculated wet-bulb temperature exceeded the 90th percentile of the multi-year distribution for the corresponding period. This percentile-based approach ensures an objective statistical definition of extreme conditions. We have now added an appropriate reference for the calculation of wet-bulb temperature. The revised sentence **(L651)** now reads:

Our analysis above demonstrates that the optimization of turbulent flux parameterizations markedly enhances the accuracy of glacier surface energy and mass balance simulations under the mean climate state (e.g., multi-year averages of T_a and precipitation). However, the ability of SEB models to simulate turbulent fluxes under extreme events remains uncertain and warrants further investigation. Between 8 and 11 July, 2023, the Dunde Glacier experienced a typical humid heatwave (Dong et al., 2024).

3. The heatwave analysis (Section 5.3) is one of the strengths of this paper. To further improve this section, it is recommended to include specific quantitative data to illustrate how the anomalous turbulent flux variations during the humid heatwave affected the glacier surface energy balance, thereby strengthening the comparison with non-extreme periods.

Answer: We thank the reviewer for recognizing the importance of the heatwave analysis. In the revised manuscript, we have included detailed quantitative comparisons between the humid heatwave period (8–11 July 2023) and the non-heatwave period (the remainder of July 2023) based on quality-controlled observational data.

Specifically, during the humid heatwave, the daily mean sensible heat flux (H) increased markedly to 17.5 W m^{-2}, which is nearly 2.5 times higher than the non-heatwave average (7.5 W m^{-2}). The daily range of H (7.5–26.5 W m^{-2}) also substantially exceeded that observed during the non-heatwave period (−1.5 to 22.1 W m^{-2}), indicating enhanced atmospheric heat transfer to the glacier surface.

Concurrently, the latent heat flux (LE) exhibited a pronounced reduction in magnitude. While LE remained consistently negative during the non-heatwave period with a mean of −25.2 W m^{-2}, its magnitude decreased substantially during the humid heatwave, with a mean value of −3.1 W m^{-2} and occasional positive values (5.1 W m^{-2} on 11 July). This shift implies a weakening of upward latent heat flux and episodic moisture condensation onto the glacier surface.

As a result, the glacier surface transitioned from a state of net turbulent energy loss (−13.8 W m^{-2}) during non-heatwave conditions to net turbulent energy gain (14.4 W m^{-2}) during the humid heatwave. This clear reversal demonstrates how anomalous turbulent flux variations significantly altered the glacier's surface energy balance.

Furthermore, we linked these turbulent flux changes to enhanced melt processes, including snow metamorphism, albedo reduction, and intensified ablation. We also evaluated model performance under these extreme conditions, identifying that the CM–O + SvdB scheme most consistently reproduced the observed H enhancement, although errors in LE estimation remained non-negligible.

These quantitative analyses have been explicitly included in Section 5.3 to strengthen the comparison between extreme and non-extreme periods. The revised sentence **(L349 and L669)** now reads:

"To clarify turbulent flux behaviors under such anomalous climatic conditions, we compared turbulent fluxes during the humid heatwave (8 – 11 July, 2023) with those during the non-heatwave period (the remainder of July, 2023) based on quality-controlled observational data. The H markedly increased during the humid heatwave, reaching a daily average of 17.5 W m^{-2}, this being nearly 2.5 times higher than the non-heatwave average (7.5 W m^{-2}). Moreover, the daily variation in H during the heatwave event ranged from 7.5 to 26.5 W m^{-2}, substantially exceeding the range observed during the non-heatwave period (−1.5 to 22.1 W m^{-2}). This extraordinary increase in H during the humid heatwave indicates that substantial heat was transferred from the atmosphere to the glacier during this event. Concurrently, LE decreased during the humid heatwave period. During the non-heatwave period, LE remained negative, with an average value of −25.2 W m^{-2}. Such negative LE values are a common characteristic of continental

glaciers on the TP. However, during the humid heatwave, the absolute magnitude of LE decreased, with a mean value of −3.1 W m^{-2} (with a mean of 5.1 W m^{-2} on July 11). This change was further reflected in daily LE variations, with a range of −7.6 to 5.1 W m^{-2} during the humid heatwave, which was markedly different from the range of −58.8 to −2.6 W m^{-2} observed during the rest of July. This shift implies a weakening of the upward latent heat flux and, at times, a reversal in flux direction, reflecting enhanced moisture condensation from the atmosphere onto the glacier surface and thus increased latent heat input (Zhang et al., 2017). Such weakly negative LE values, and occasional positive values, are more commonly observed over maritime glaciers and in high-latitude Arctic regions. In maritime settings, they are primarily associated with relatively high air temperatures and abundant precipitation, whereas in Arctic regions they are linked to weak solar radiation, which may occasionally cause glacier surface temperatures to fall below air temperature (Kuipers Munneke et al., 2009, 2018; Yang et al., 2011).

The glacier surface transitioned into a state of net turbulent energy gain, with the mean total turbulent flux (LE + H) reaching 14.4 W m^{-2} during the humid heatwave. In contrast, the non-heatwave period in July was characterized by net turbulent energy loss, averaging −13.8 W m^{-2}. This contrast underscores a distinct shift from turbulent heat loss to heat gain under humid heatwave conditions. Concurrently, rising T_a during the humid heatwave promoted snowmelt on the glacier surface, leading to rapid snow metamorphism characterized by grain growth and rounding. As the humid heatwave persisted, continued melting may have locally removed portions of the seasonal snow cover, potentially exposing underlying ice. This reduction in surface albedo enhanced melt energy, triggering intense ablation (Fig. 8c). Thus, although short-lived, such anomalous turbulent flux variations during the humid heatwave markedly altered the glacier's energy-balance processes by modifying albedo and melt energy, with potential implications for longer-term melt dynamics (Zhu et al., 2024b).

We further evaluated the ability of the five methods to simulate turbulent fluxes under extreme weather events. Among the five turbulent flux methods tested, all captured the pronounced increase in H during the humid heatwave, with the C_{Rib1} and

C_{M-O} schemes combined with the SvdB scalar roughness length parameterization performing best. Although the mean values simulated by C_{Rib1} + SvdB and C_{M-O} + SvdB (16.7 and 16.4 W m^{-2}, respectively) were slightly lower than the observed value (17.5 W m^{-2}), their performance was still superior to that of the other schemes. The C_{kat} method exhibited the poorest performance, simulating a mean H of only 7.9 W m^{-2}. Meanwhile, the mean H values during the humid heatwave simulated by the C_{log}, C_{Rib1} + A87, C_{Rib2} and C_{M-O} + A87 methods were 12.7, 14.3, 14.7, and 14.4 W m^{-2}, respectively. For LE, all methods exhibited noticeable deviations from the observations. Among the five evaluated methods, the C_{kat} scheme performed relatively better, with a mean value of −9.2 W m^{-2}, which may be related to its generally lower simulated fluxes throughout the study period. The next best performance was obtained by the C_{M-O} + A87 scheme, with a mean value of −11.6 W m^{-2}. The remaining methods showed broadly similar results: the mean LE values simulated by C_{log}, C_{Rib1} + A87, C_{Rib1} + SvdB, C_{Rib2}, and C_{M-O} + SvdB were −16.0, −14.1, −16.2, −14.1, and −13.0 W m^{-2}, respectively, all substantially deviating from the observed value of −3.1 W m^{-2}. Overall, the methods, particularly the C_{M-O} + SvdB scheme, reproduced the anomalous increase in H during the humid heatwave with relatively high consistency and accuracy, and captured the decreasing tendency of LE during this period. However, the estimation errors for LE were non-negligible, and the models failed to reproduce the occasional reversal in LE direction (on July 11). Part of the discrepancy between modeled and observed results may be attributed to observational limitations. The meteorological variables used to drive the models are based on half-hourly observations. Such temporal averaging may obscure short-lived near-surface temperature and humidity gradients, thereby limiting the models' ability to reproduce transient fluctuations. Nevertheless, the discrepancies in turbulent fluxes identified in this study suggest that current parameterization schemes may underestimate the mass loss driven by LE under extreme meteorological conditions, thereby underestimating its role in glacier melt processes.

Under ongoing global warming, the climate system is recording notable warming and moistening trends on the TP (Wang et al., 2010). This means that the TP will likely experience an increased frequency and intensity of humid heatwave events (Zhang et

al., 2025). Such conditions will cause continental glaciers, such as the Dunde Glacier, to increasingly exhibit turbulent flux characteristics that resemble those of maritime glaciers, including reduced LE magnitudes and even reversals in LE direction, as well as a pronounced enhancement of H. This phenomenon warrants further investigation and is likely related to the constraint that T_s cannot exceed 0 °C. Under humid heatwave conditions, T_a continues to rise while T_s is capped, leading to an increased surface temperature deficit and consequently a substantial enhancement of H. Meanwhile, because the humidity gradient is closely coupled to the temperature gradient, LE may also undergo anomalous changes. Consequently, continued warming may drive future transitions in glacier types."